BEST AVAILABLE IMAGES

Defective images within this document are accurate representations of the original documents submitted by the applicant.

Defects in the images may include (but are not limited to):

- BLACK BORDERS
- TEXT CUT OFF AT TOP, BOTTOM OR SIDES
- FADED TEXT
- ILLEGIBLE TEXT
- SKEWED/SLANTED IMAGES
- COLORED PHOTOS
- BLACK OR VERY BLACK AND WHITE DARK PHOTOS
- GRAY SCALE DOCUMENTS

IMAGES ARE BEST AVAILABLE COPY.

As rescanning documents *will not* correct images, please do not report the images to the Image Problem Mailbox.

Exhibit 1

Volume 48(8): 1059–1077, 2000
The Journal of Histochemistry & Cytochemistry
http://www.jhc.org

ARTICLE

A Histomorphometric, Structural, and Immunocytochemical Study of the Effects of Diet-induced Hypocalcemia on Bone in Growing Rats

P. Mocetti, P. Ballanti, S. Zalzal, G. Silvestrini, E. Bonucci, and A. Nanci

Department of Experimental Medicine and Pathology, Università "La Sapienza," Rome, Italy (PM,PB,GS,EB); and Laboratory for the Study of Calcified Tissues and Biomaterials, Université de Montréal, Montreal, Quebec, Canada (PM,SZ,AN)

SUMMARY Despite several studies on the effect of calcium deficiency on bone status, there is relatively little information on the ensuing histological alterations. To investigate bone changes during chronic hypocalcemia, weanling rats were kept on a calcium-free diet and deionized water for 28 days while control animals were fed normal chow. The epiphyseal–metaphyseal region of the tibiae were processed for histomorphometric, histochemical, and structural analyses. The distribution of bone sialoprotein (BSP), osteocalcin (OC), and osteopontin (OPN), three noncollagenous bone matrix proteins implicated in cell–matrix interactions and regulation of mineral deposition, was examined using postembedding colloidal gold immunocytochemistry. The experimental regimen resulted in serum calcium levels almost half those of control rats. Trabecular bone volume showed no change but osteoid exhibited a significant increase in all its variables. There were a multitude of mineralization foci in the widened osteoid seam, and intact matrix vesicles were observed in the forming bone. Many of the osteoblasts apposed to osteoid were tartrate-resistant acid phosphatase (TRAP)- and alkaline phosphatase-positive, whereas controls showed few such TRAP-reactive cells. Osteoclasts in hypocalcemic rats generally exhibited poorly developed ruffled borders and were inconsistently apposed to bony surfaces showing a lamina limitans. Sometimes osteoclasts were in contact with osteoid, suggesting that they may resorb uncalcified matrix. Cement lines at the bone–calcified cartilage interface in some cases were thickened but generally did not appear affected at bone–bone interfaces. As in controls, electron-dense portions of the mineralized matrix showed labeling for BSP, OC, and OPN but, in contrast, there was an abundance of immunoreactive mineralization foci in osteoid of hypocalcemic rats. These data suggest that chronic hypocalcemia affects both bone formation and resorption. (J Histochem Cytochem 48:1059–1077, 2000)

KEY WORDS
rat
bone
hypocalcemia
hyperparathyroidism
osteomalacia
histomorphometry
TRAP
alkaline phosphatase
bone sialoprotein
osteocalcin
osteopontin
cement line

CALCIUM plays an important role in cellular physiology and homeostasis. It is stored when bone is deposited and liberated when it is resorbed. The serum calcium level is a major factor regulating bone remodeling (reviewed in Dempster 1992). The use of calcium-deficient diets to investigate the effect of hypocalcemia on bone has generated variable results. Among the various changes reported to be induced by calcium deprivation one finds (a) low levels of bone formation, bone loss, or even diffuse osteoporosis (Jowsey and Gershon–Cohen 1964; Salomon and Volpin 1970; Salomon 1972; Stauffer et al. 1973; Ornoy et al. 1974; de Winter and Steendijk 1975; Sissons et al. 1984; Ohya 1994; Shen et al. 1995), (b) a rise in number of osteoclasts and in degree of bone resorption (Bloom et al. 1958; Stauffer et al. 1973; Thompson et al. 1975; Liu et al. 1982; Liu and Baylink 1984; Ohya 1994), (c) an increase in the number of endosteal cells (Bloom et al.

Correspondence to: Dr. Antonio Nanci, Université de Montréal, Faculty of Dentistry/Stomatology, PO Box 6128, Station Centre-Ville, Montreal, QC, Canada H3C 3J7. E-mail: nancia@ere.umontreal.ca

Received for publication October 30, 1999; accepted March 15, 2000 (9A5113).

0022-1554/00/$3.30

Table 1 Serum values of calcium, phosphorus, albumin, creatinine, alkaline phosphatase, aspartate aminotransferase and alanine aminotransferase reported as mean ± SD[a]

Groups	Ca	P	ALB	CRE	AP	AlAT	AsAT
Hypocalcemic	1.38 ± 0.08*	3.87 ± 0.60	23.46 ± 2.55	55.73 ± 13.43	399.8 ± 97.0*	79.53 ± 22.43*	198.53 ± 71.79
Control	2.84 ± 0.10	3.79 ± 0.35	22.87 ± 0.99	54.00 ± 15.41	225.5 ± 66.3	27.62 ± 8.63	151.87 ± 40.71

[a]Ca, calcium (mmol/liter); P, phosphorus (mmol/liter); ALB, albumin (g/liter); CRE, creatinine (μmol/liter); AP, alkaline phosphate, (IU/liter); AsAT, aspartate aminotransferase (IU/liter); AlAt, alanine aminotransferase (IU/liter).
*$p<0.001$ vs. controls.

1958; Stauffer et al. 1973), and (d) in young, growing animals, the presence of severe calcification defects similar to those observed in rickets and osteomalacia (Bloom et al. 1958; Stauffer et al. 1973; de Bernard et al. 1980; Pettifor et al. 1984).

The aim of the present investigation was to clarify, using a combination of morphological approaches, the changes in bone status induced by chronic hypocalcemia in growing rats, an animal model frequently used to study the effects of metabolic factors on bone and bone cells (Salomon 1972; Stauffer et al. 1972,1973; de Winter and Steendijk 1975; Liu and Baylink 1984; Ohya 1994). Static histomorphometry, histochemical, structural, and immunocytochemical analyses were applied to characterize the histological and extracellular matrix alterations in tibial metaphyseal spongy bone of animals fed a calcium-free diet.

Materials and Methods

Hypocalcemic Diet

Eighteen 21-day-old Wistar rats weighing about 45 g (Charles River; St-Constant, QC, Canada) were maintained on a cycle of 12-hr light/12-hr dark and were fed a completely calcium-free diet (Altromin DP1031; Rieper, Vandois, Italy) for 28 days. Another eight rats were used as controls and were given a normocalcemic diet (Altromin DP1000; Rieper) for the same period of time. The animals had free access to food and deionized water. Both the calcium-free and the normocalcic food contained 1000 IU of vitamin D/kg. An additional group of three rats was treated for 28 days with Altromin DP1031 containing 2500 IU of vitamin D/kg of food to rule out the possibility that the alterations observed reflected a vitamin D-dependent rickets. The experimental protocol was approved by the Comité de Déontologie de l'Expérimentation sur les Animaux of the Université de Montréal.

Blood Sampling and Tissue Processing for Histological Analyses

On Day 28, the rats were anesthetized with chloral hydrate (Sigma Chemical; St Louis, MO) and blood samples were drawn from the jugular vein for routine biochemical assays of (a) calcification parameters (calcium, phosphorus, alkaline phosphatase), (b) renal function (creatinine), (c) intestinal protein absorption (albumin), and (d) liver activity (aspartate aminotransferase and alanine transferase). The rats were then perfused through the left ventricle with lactated Ringer's solution (Abbott; Montreal, QC, Canada) for about 30 sec, followed by fixative for 20 min. The fixative solution consisted of either 4% paraformaldehyde + 0.1% glutaraldehyde in 0.08 M sodium cacodylate buffer, pH 7.3, or 1% glutaraldehyde in the same buffer. After perfusion, the tibiae were dissected, split longitudinally, and immersed in the corresponding fresh fixative solution for 3 hr (paraformaldehyde–glutaraldehyde) or overnight (glutaraldehyde) at 4C. The proximal metaphysis of each hemitibia was then dissected and subdivided into small segments. These were processed for embedding in glycolmethacrylate (Merck/Schuchardt; Darmstadt, Germany) for enzyme histochemistry (Bianco et al. 1984) or LR White acrylic resin (Mecalab; Pointe-aux-Trembles, QC, Canada) for postembedding colloidal gold immunolabeling (Bendayan et al. 1987; Nanci et al. 1989). Some of the specimens were decalcified with 4.13% (ethylenedinitrilo)tetraacetic acid (EDTA, disodium salt), pH 7.2, for 2 weeks at 4C before embedding (War-

Table 2 Histomorphometric values (mean ± SD) for bone structural parameters[a]

	BV/TV	Tb.Th	Tb.N	Tb.Sp	G.P.Wi
Hypocalcemic	9.69 ± 3.43	36.12 ± 3.22	2.63 ± 0.75	384 ± 127	581 ± 116
Vitamin D-supplemented	9.67 ± 0.54	31.19 ± 0.18	3.11 ± 0.18	292 ± 20	594 ± 43
Control	9.55 ± 1.81	40.57 ± 3.40	2.34 ± 0.32	297 ± 70	556 ± 61
ANOVA	NS	$p<0.008$	NS	NS	NS
Hypocalcemic vs control,		$p<0.02$			
Hypocalcemic vs vitamin D-supplemented,	NS				
Control vs vitamin D-supplemented,		$p<0.003$			

[a]BV/TV, % of total volume occupied by bone; Tb.Th, trabecular thickness in μm; Tb.N, trabecular number; Tb.Sp, trabecular separation in μm; G.P.Wi, growth plate width in μm.
*Student's *t*-test within ANOVA.

Table 3 Histomorphometric values (mean ± SD) for bone formation-associated indices[a]

	OV/BV	O.Th	OS/BS	Ob.S/BS
Hypocalcemic	68.06 ± 6.37	17.62 ± 2.86	70.24 ± 4.14	67.43 ± 4.84
Vitamin D-Supplemented	49.37 ± 6.45	10.02 ± 0.71	70.91 ± 4.42	70.91 ± 4.42
Control	4.18 ± 0.24	2.21 ± 0.56	37.04 ± 6.54	35.25 ± 6.88
ANOVA	<0.000	<0.000	<0.000	<0.000
Hypocalcemic vs control*	$p<0.000$	$p<0.000$	$p<0.000$	$p<0.000$
Hypocalcemic vs vitamin D-supplemented*	$p<0.000$	$p<0.0001$	NS	NS
Control vs vitamin D-supplemented*	$p<0.000$	$p<0.0002$	$p<0.000$	$p<0.000$

[a]OV/BV, % bone volume occupied by osteoid; O. Th, osteoid thickness in μm; OS/BS, % bone surface occupied by osteoid; Ob. S/BS, % of bone surface occupied by osteoblasts.
*Student's *t*-test within ANOVA.

shawsky and Moore 1967). Other undecalcified specimens were postfixed with potassium ferrocyanide-reduced osmium tetroxide (Neiss 1984) and embedded in Epon for routine light and electron microscopic examination.

Histomorphometric Analysis

Histomorphometric analysis of undecalcified tibiae was carried out with an interactive image analyzer (IAS 2000; Delta Sistemi, Rome, Italy) on at least three ~2-μm-thick sections from each animal. The sections were cut at intervals of ~60 μm with a Reichert-Jung 1150/Autocut microtome. Structural variables (for nomenclature see Parfitt et al. 1987) were measured in the spongiosa within a conventional 1.11 × 2.29-mm (2.54 mm^2) rectangular window whose upper side was centered 1 mm below the growth plate–metaphyseal junction. Remodeling variables were analyzed in the same region using a 0.85 × 1.02-mm (0.87 mm^2) window. Growth plate width was measured at five equally spaced distances. Differences between groups were assessed by the bidirectional *t*-test adjusted for multiple comparison. The test was performed after assessment of significant difference by one-way analysis of variance (ANOVA). Statistical significance was considered at $p<0.05$.

Cytochemical Staining

Thick sections for light microscopy were stained with azure II–methylene blue for routine examination or by the von Kossa method for calcium phosphate. Glycolmethacrylate sections were used to demonstrate alkaline phosphatase (AP) and tartrate-resistant acid phosphatase (TRAP) activities under the light microscope (Bianco and Bonucci 1991). TRAP activity was also visualized at the ultrastructural level using cerium-based preembedding cytochemistry and epoxy resin embedding (Robinson and Karnovsky 1983; Clark et al. 1989; Bonucci et al. 1992). Some glycolmethacrylate sections stained with azure II–methylene blue or by the von Kossa method were also used for histomorphometry.

Immunolocalization of Noncollagenous Bone Matrix Proteins

Postembedding protein A–colloidal gold immunolabeling of tissue sections was applied to examine the presence and distribution of bone sialoprotein (BSP), osteocalcin (OC), and osteopontin (OPN) (reviewed in Bendayan 1995; McKee and Nanci 1995). Briefly, decalcified and undecalcified grid-mounted LR White tissue sections were blocked for 15 min by floating on a drop of 0.01 M PBS containing 1% ovalbumin (Sigma). They were then incubated with chicken egg yolk anti-rat OPN antibody (1:150 for 3 hr; Nanci et al. 1996) followed by rabbit anti-chicken IgG antibody (Cappel; Organon Teknika, Scarborough, ON, Canada), goat anti-rat OC (1:50; Hauschka et al. 1983), or with rabbit anti-rat BSP (1:100 for 3 hr; LF-87; Midura et al. 1990). After incubation with antibody, sections were rinsed with PBS, placed on a drop of PBS–1% ovalbumin for 15 min, and then floated on a drop of protein A–gold complex (dilution 1:25) for 30 min. The complex was prepared as described in Bendayan (1995) using colloidal gold particles of ~8 nm (Frens 1973). All incubations were carried out at room temperature. Controls were incubated with the secondary antibody followed by protein A–gold or protein A–gold alone. Sections were finally washed with PBS, rinsed with distilled

Table 4 Histomorphometric values (mean ± SD) of bone resorption-associated indices[a]

	ES/BS	Oc.S/BS	Oc.N/BS
Hypocalcemic	25.64 ± 3.07	20.08 ± 3.38	9.54 ± 2.01
Vitamin D-supplemented	22.38 ± 0.87	19.02 ± 1.03	9.44 ± 0.63
Control	20.76 ± 2.31	19.65 ± 1.93	7.75 ± 0.79
ANOVA	p<0.01	NS	NS
Hypocalcemic vs control*	p<0.004		
Hypocalcemic vs vitamin-supplemented*	NS		
Control vs vitamin-supplemented*	NS		

[a]ES/BS, % ob bone surface showing erosion; Oc.S/BS, % of bone surface occupied by osteoclasts; Oc. N/BS number of osteoclasts/mm^2.
*Student's *t*-test within ANOVA.

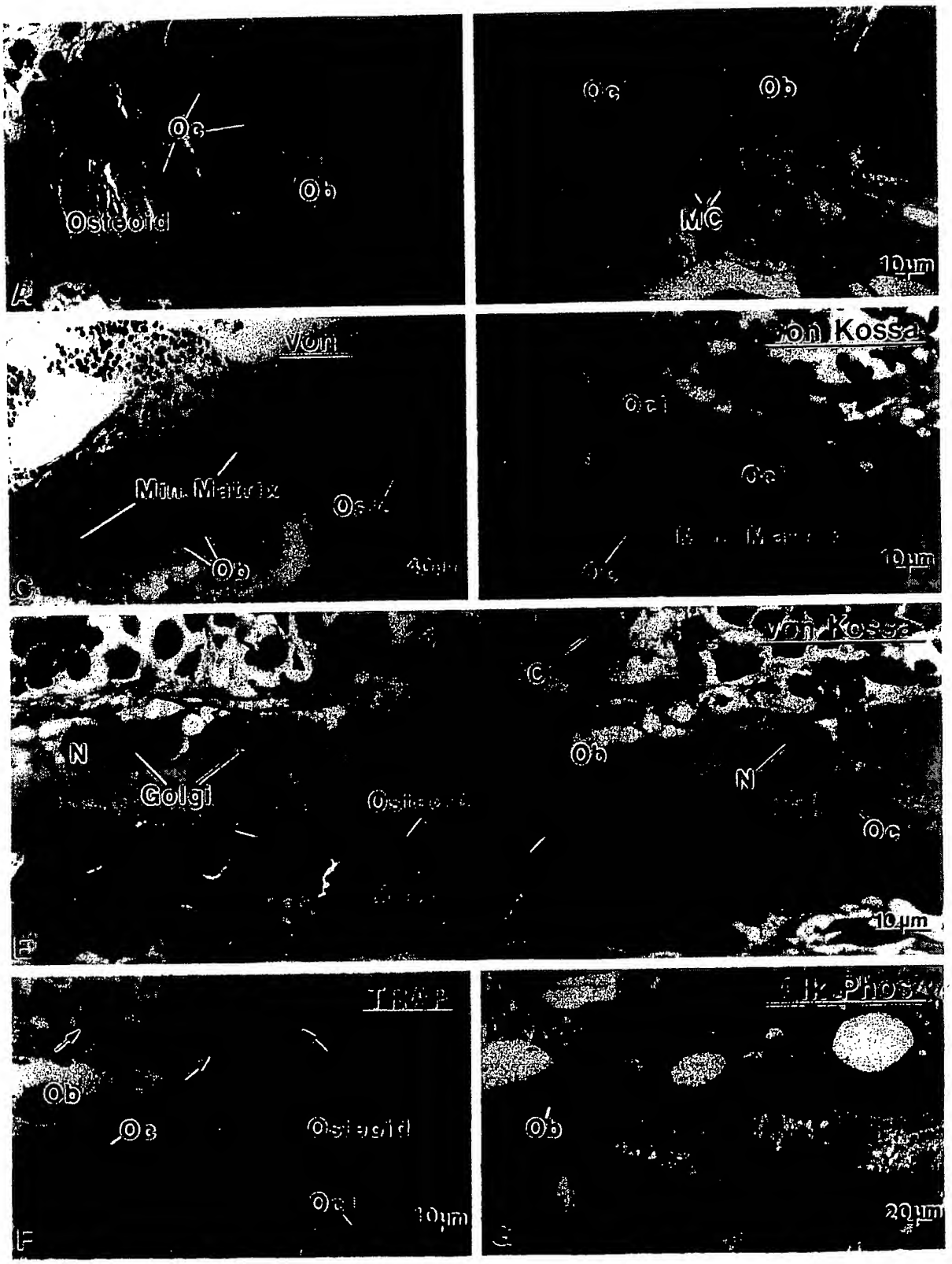
Oc
Ob
Osteoid
MC
10μm
Von
Mineralized Matrix
Oc
Ob
40μm
Von Kossa
Oc
Ob
10μm
Von Kossa
C
N
Golgi
Osteoid
Ob
N
Oc
10μm
TRAP
Ob
Oc
Osteoid
Oc
10μm
Alk Phosp
Ob
20μm

water, stained with uranyl acetate and lead citrate, and examined in a JEOL 1200EX-II transmission electron microscope operated at 60 kV.

Results

Animals from the present study (except for the hypocalcemic group supplemented with vitamin D) were also used to examine enamel formation in the mandibular incisors. Details of food and water consumption, and weight progression for the hypocalcemic and control groups are given in Nanci et al. (2000). The average weight of hypocalcemic rats after 28 days was 124 ± 11.6 g compared to 244.9 ± 49.2 for controls.

Biochemical Assays

Results of the blood analyses are summarized in Table 1. The serum data showed conspicuous hypocalcemia in calcium-deprived rats (1.38 ± 0.09 vs 2.8 ± 0.10 mmol/liter; $p<0.001$), an increase in alkaline phosphatase and alanine aminotransferase, and normal values for phosphorus, creatinine, albumin, and aspartate aminotransferase.

Histomorphometry

The bone volume of calcium-deficient rats showed no significant difference from that of control rats (Table 2). Animals given a supplement of vitamin D (2500 IU of vitamin D) exhibited similar values. The absence of calcium in the diet resulted in a significant reduction of trabecular thickness, compared to the control group. The growth plate width was similar in three groups.

Both groups of rats given a calcium-free diet showed a significant increase in the osteoid parameters with respect to controls, as indicated by the values for osteoid volume, osteoid thickness, and osteoid surface (Table 3). Of note is that osteoid volume and thickness increased less in rats fed on a diet with 2500 IU/kg of vitamin D than in those maintained on a diet containing 1000 IU/kg. In both groups the osteoblast surface was also significantly greater than that in controls.

Osteoclast surface and osteoclast number were not significantly altered by hypocalcemia (Table 4). The eroded surface was significantly higher in treated rats receiving 1000 IU of vitamin D but not in those fed a diet with 2500 IU. However, in both these groups, almost all trabecular surfaces showed signs of bone remodeling.

Histology

The metaphyses of hypocalcemic rats appeared to consist of rather irregular trabeculae, delimiting medullary spaces that contained dilated capillary vessels and hemopoietic cells. Very few trabeculae were lined by typical bone lining cells, the majority of endosteal surfaces being covered by well-developed osteoblasts (Figures 1A and 1B). Many osteoclasts were observed along the bone surfaces and mast cells were abundant near bone (Figures 1B, 1D, and 1E). Osteoclasts, particularly those near the growth plate, were often found apposed to unmineralized matrix (Figure 1D). The organization of osteoblasts along trabeculae varied according to the distance from the growth plate cartilage. Those at a distance generally formed a single row (Figures 1C and 1E), whereas those nearer the growth plate appeared to be hyperplastic (Figure 1A). In both cases, the cells were rather large (mean diameter about 15 μm), and showed a deeply stained cytoplasm with a conspicuous Golgi apparatus and an eccentric nucleus with one or two nucleoli (Figures 1A and 1E). Von Kossa staining confirmed that the central part of the trabeculae was calcified, whereas the peripheral bone matrix consisted of thick, uncalcified osteoid borders with a widened seam showing many mineralization foci (Figures 1C and 1E).

Enzyme Histochemistry

In hypocalcemic rats, the majority of osteoclasts were TRAP-positive, and intensely reactive mononuclear

Figure 1 Sections of glycolmethacrylate-embedded mineralized tibiae from hypocalcemic rats. **(A)** Near the growth plate, the metaphyseal trabeculae consist mainly of osteoid matrix lined by many osteoblasts. Azure II–methylene blue. **(B)** Portion of a metaphyseal trabecula showing an osteoclast (Ocl) and many osteoblasts (Ob) in a Howship's lacuna. Note the presence of many mast cells (MC) near the bone surface. Azure II–methylene blue. **(C)** Bone shows an abundance of osteoid tissue and a paucity of mineralized matrix (Min. Matrix), as illustrated in this metaphyseal trabecula situated away from the growth plate. At this site, osteoblasts lining the bone surface generally form a single row of cells. von Kossa. **(D)** Osteoclasts are apposed to both the uncalcified osteoid border and mineralized matrix. Note the presence of well-developed osteocytes (Oc) in both these matrices. von Kossa. **(E)** Higher magnification, showing a trabecula with a thick layer of osteoid and a relatively thin layer of mineralized matrix. Note the widened osteoid seam (arrowheads) characterized by the presence of many mineralization foci and the abundance of mast cells near the forming bone surface. von Kossa. **(F)** Tartrate-resistant acid phosphatase staining (TRAP); note the intense reaction in osteoclasts and in mononuclear cells (arrows) in the tissue surrounding the trabecula. Osteoblasts and osteocytes are less reactive and show granular deposits of reaction product, particularly at the interface between osteoblasts and the osteoid tissue. **(G)** Alkaline phosphatase (Alk Phos) staining; osteoblasts show enzyme activity along their plasma membrane.

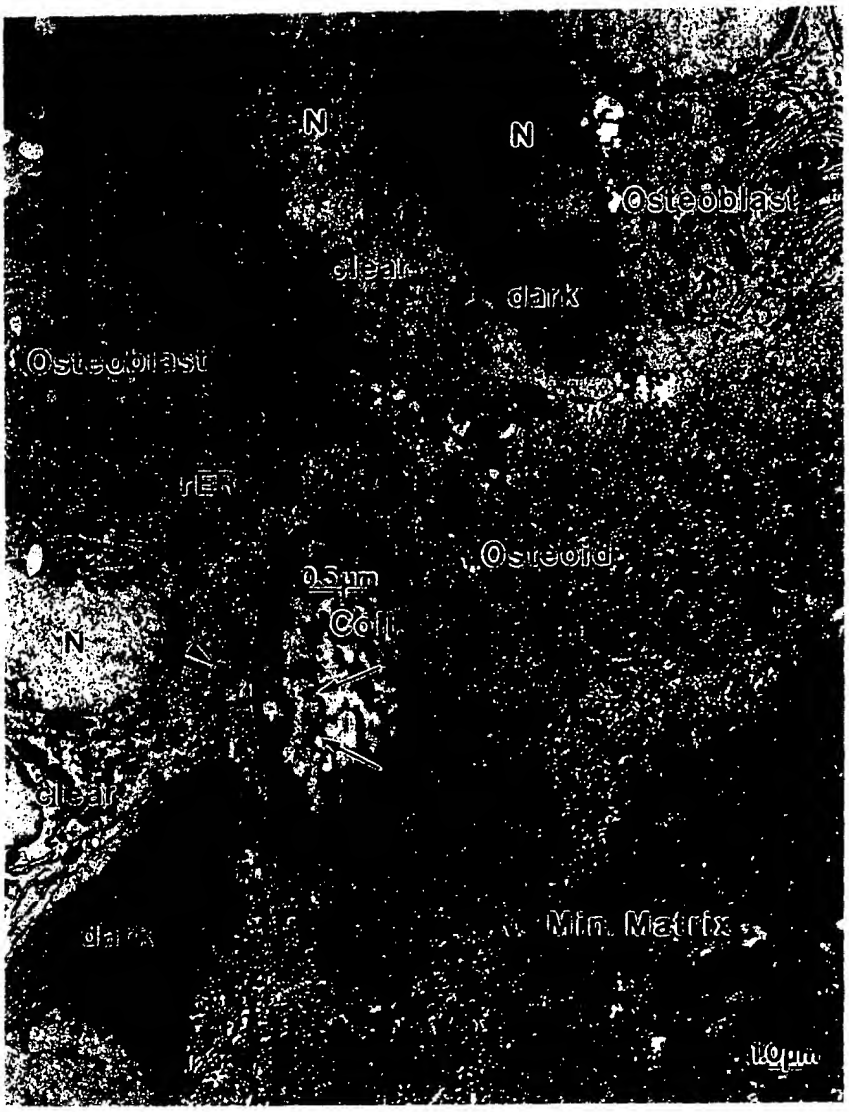

Figure 2 Electron micrograph illustrating part of a metaphyseal trabecula from a hypocalcemic rat. The mineralized bone matrix (Min. Matrix) is surrounded by a thick layer of osteoid. A variety of mononuclear cells are apposed to it. Typical osteoblasts are generally cuboidal and show a prominent Golgi apparatus (Golgi), occupying much of the cytoplasm. (Inset) Coated pits (arrows) are present along the plasma membrane facing the osteoid. The other two cell types are more elongated and exhibit an inconspicuous Golgi apparatus. One shows a "clear" cytoplasm whereas the other is "dark" and its cytoplasm is mainly occupied by rough endoplasmic reticulum (rER). N, nucleus.

cells were frequently seen around them (Figure 1F). TRAP activity was also present in osteoblasts and osteocytes (Figure 1F). The reaction product in these cells appeared as granular deposits which, in the case of osteoblasts, were aligned along the cell membrane facing osteoid (Figure 1F). Practically all the osteoblasts along the metaphyseal trabeculae showed TRAP staining, whereas those lining diaphyseal bone or the diaphyseal terminal portion of trabeculae were, in general, very weakly or not reactive. Osteoblasts also showed strong alkaline phosphatase activity. The reaction product was localized along their cell membrane (Figure 1G). In control animals, the majority of osteoblasts were TRAP-negative, reaction product being found only in some cells lining the initial portion of the trabeculae near calcifying cartilage, but all osteoblasts exhibited membrane-bound alkaline phosphatase (data not shown).

Electron Microscopy

The metaphyseal trabeculae of hypocalcemic rats consisted of a central calcified zone surrounded by a thick layer of osteoid showing abundant calcification foci (Figure 2). The trabeculae were lined by a variety of mononuclear cells (Figure 2). Many of them showed ultrastructural characteristics similar to those reported for active osteoblasts (Scherft and Groot 1990). They

were generally cuboidal in shape and possessed a roundish nucleus with dispersed chromatin and one or two nucleoli. A large part of the cytoplasm was occupied by the Golgi apparatus (Figures 2, 3, and 4), whereas the remaining portion contained cisternae of the rough endoplasmic reticulum, mitochondria, lysosome-like bodies, and a number of vesicles of variable electron density (Figures 2, 3, and 4). The plasma membrane was generally smooth but coated pits were occasionally seen facing the osteoid (Figure 2, inset). These osteoblasts showed few cell processes but there were many vesicular profiles among the irregularly oriented collagen fibrils of the adjacent osteoid layer (Figure 3). Some of the lining cells showed a clear cytoplasm, contained few protein synthetic organelles, and extended thick cytoplasmic processes into the osteoid matrix (Figure 2). A third mononuclear cell type was also associated with osteoid; it was more electron-dense, contained an ovoid nucleus, and was rich in rough endoplasmic reticulum but showed no extensive Golgi apparatus (Figure 2).

Osteoclasts in calcium-deficient rats showed either well-developed or incomplete ruffled borders and contacted either calcified and/or uncalcified bone matrix (Figures 5–7). They appeared to be less frequently apposed to bone surfaces showing a lamina limitans (Figures 5–7) (see Nanci et al. 1994,2000 for discussion on the use of the terms cement line and lamina limitans). In many cases, the osteoclasts contacted the bone surface via extensions that intruded between typical osteoblasts or mononucleated clear cells with a paucity of protein synthetic organelles (Figure 7). Crystallites were also sometimes present deep among the membrane infolding of cells with seemingly normal ruffled borders (Figure 5B, inset). Intact collagen fibrils or recognizable fragments were not observed intracellularly within cytoplasmic vacuoles of the control and hypocalcemic rats examined.

Ultrastructural Cytochemistry

Osteoclasts in hypocalcemic rats showed TRAP activity, even those in direct contact with osteoid tissue (Figure 8). Reaction product was localized in small electron-lucent vesicles in the region of the ruffled border and in larger lysosome-like profiles (Figure 8). Some reactivity was also found along the outer membrane of mitochondria (Figure 8).

Although many TRAP reaction product deposits were seen in osteoblasts by light microscopy, relatively few reactive granules were noted at the ultrastructural level, a situation probably due to the fact that the granules are small and are distributed throughout the large cell volume (Figure 9). However, systematic analysis of several serial sections revealed the presence of TRAP-positive vacuoles in the majority of osteoblasts from hypocalcemic rats.

Immunocytochemistry

Control rats showed a distribution for BSP, OC, and OPN similar to what has been previously reported for normal animals (data not shown; Bianco et al. 1993; McKee et al. 1993; McKee and Nanci 1995,1996; Riminucci et al. 1995), i.e., over mineralization foci at the osteoid seam, patches of matrix among the mineralized collagen fibrils, and over cement lines and laminae limitantes. In rats fed a calcium-free diet, immunolabeling for BSP and OPN was found over these same extracellular matrix compartments (Figures 4–7 and 10–12). Although labeling for OC was also found over electron-dense portions of bone matrix, in some areas it also showed a more diffuse distribution (Figure 5). The thickened osteoid layer showed abundant mineralization foci immunoreactive with all three antibodies (Figures 6 and 10–12). Cement lines at the mineralized bone–cartilage interface and between older and younger bone were typically immunoreactive (Figures 10–12). In many cases, the interfacial layer between bone and cartilage was thicker than in normal rats (Figure 11B). Occasionally, patches of OPN-immunoreactive matrix were seen within pit-like membrane inpocketings of osteoclasts showing a poorly-developed ruffled border (Figure 5A, inset). Matrix vesicles in osteoid were not labeled (Figure 10D). It is noteworthy that in both hypocalcemic and normal rats, immunolabeling for noncollagenous matrix proteins among the mineralized collagen showed dramatic variations and that areas with almost no immunoreactivity were frequently found adjacent to normally labeled ones (discussed in Nanci 1999).

Discussion

In this study we applied a combination of morphological approaches to examine the effects of diet-induced chronic hypocalcemia in young, growing rats. Calcium deficiency in these animals produced severe bone alterations characterized by an increase in osteoid but no change in thickness of the growth plate. These data are consistent with some previous reports indicating that hypocalcemia induces calcification defects similar to those observed in rickets and osteomalacia (Bloom et al. 1958; Stauffer et al. 1973; de Bernard et al. 1980; Pettifor et al. 1984). Vitamin D is probably not a major contributor to the resulting alterations because there was only a partial change in osteoid parameters when doses were raised from 1000 to 2500 IU. In addition, low plasma calcium would be expected to lead to an increase of 1α-hydroxylase activity in the kidney and a concomitant increase in $1,25(OH)_2D_3$ (Persson

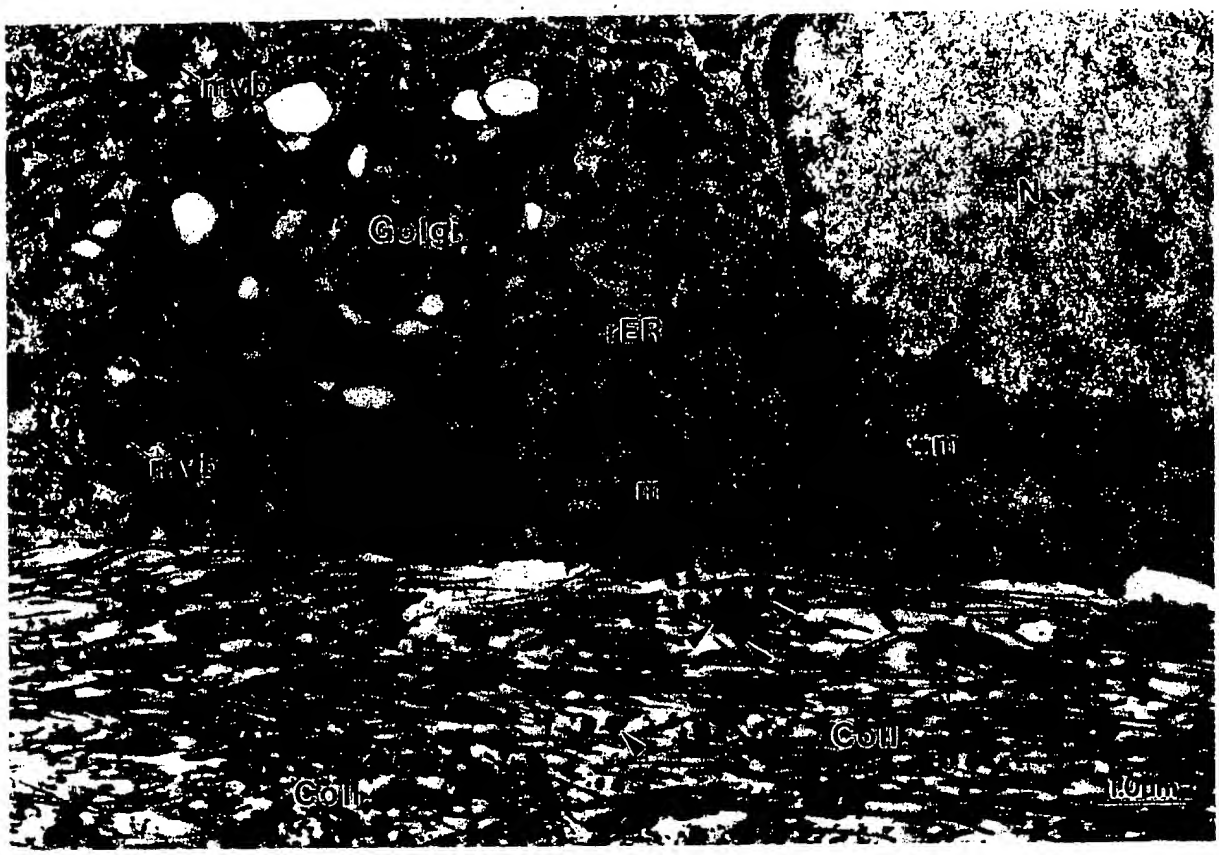

Figure 3 Higher magnification of an osteoblast from a hypocalcemic rat showing an eccentric nucleus (N) and a well-developed Golgi apparatus (Golgi). The cell is apposed to osteoid characterized by an abundance of matrix vesicle-like granules (arrowheads) and irregularly oriented collagen fibrils (Coll.). m, mitochondria; mvb, multivesicular body.

et al. 1993). Taken together, the data suggest an increase in remodeling rate which, in growing rats, may more readily lead to compensatory secondary hyperparathyroidism-like bone changes, including an accumulation of osteoid (Parfitt 1990). They are also in agreement with results from a study carried out on baboons, which revealed that diets low in both calcium and phosphorus lead to osteomalacia, whereas those low only in calcium induce hyperparathyroidism (Pettifor et al. 1984).

There are few reports in the literature in which the effects of hypocalcemia were corroborated by histomorphometric measurements, and these generally show a reduction in trabecular bone volume, especially in adult animals (Thomas et al. 1991; Weinreb et al. 1991; Shen et al. 1995). The present analysis in growing rats revealed no significant change in trabecular bone volume. Therefore, it is possible that the effect of hypocalcemia on this parameter is age-dependent. Moreover, some studies have used reduced amounts of calcium in the diet, rather than complete absence, as in the present study. The amount of calcium in the food is clearly expected to have an impact on serum calcium levels and may therefore also account for the discrepancies in bone volume observed in the various studies.

All three noncollagenous bone matrix proteins examined were immunodetected in hypocalcemic rats. There were no major changes in their pattern of distribution or concentration at labeled sites that could be inferred from qualitative observation. Immunocytochemically, the most conspicuous difference in labeling between hypocalcemic and control rats was the presence of many mineralization foci, intensely immunoreactive for BSP, OC, and OPN, in the thickened osteoid. Despite the abundance of matrix vesicles, the presence of these foci indicates that initiation of mineralization must have occurred; however, its progression was clearly hampered. The abundance of osteoid tissue and the intense immunolabeling for noncollagenous matrix proteins in mineralization foci further suggest that the reduced availability of calcium, rather than an incompetent organic matrix, is the major factor for the alteration in mineralization observed in hypocalcemic rats.

Figure 4 Immunocytochemical preparation with anti-osteopontin (OPN) antibody, showing an osteoblast near calcified cartilage. The Golgi apparatus (Golgi) of the cell shows the characteristic cylindrical (cd) and spherical distensions (sd). The cement line (CL) at the bone–cartilage interface is intensely immunoreactive. N, nucleus; rER, rough endoplasmic reticulum.

The bone changes observed appear to be independent of abnormalities of kidney, liver, or intestine, at least so far as can be inferred from the normal levels of albumin and creatinine. Total plasma alkaline phosphatase levels were increased, suggesting an increase in bone formation. This value includes both bone and liver alkaline phosphatase. However, liver damage can be excluded because, despite the significant increase in alanine aminotransferase level in hypocalcemic rats, the aspartate aminotransferase/alanine aminotransferase ratio in these animals still remained greater than 1.

The presence of abundant rough endoplasmic reticulum, a conspicuous Golgi apparatus, and alkaline phosphatase activity along the membrane of many mononuclear cells lining the osteoid surface indicates that these cells belong to the osteoblast lineage. However, detection of TRAP reactivity in many of these lining cells suggests that they are also actively involved in degradative functions. TRAP-positive osteoblast-like

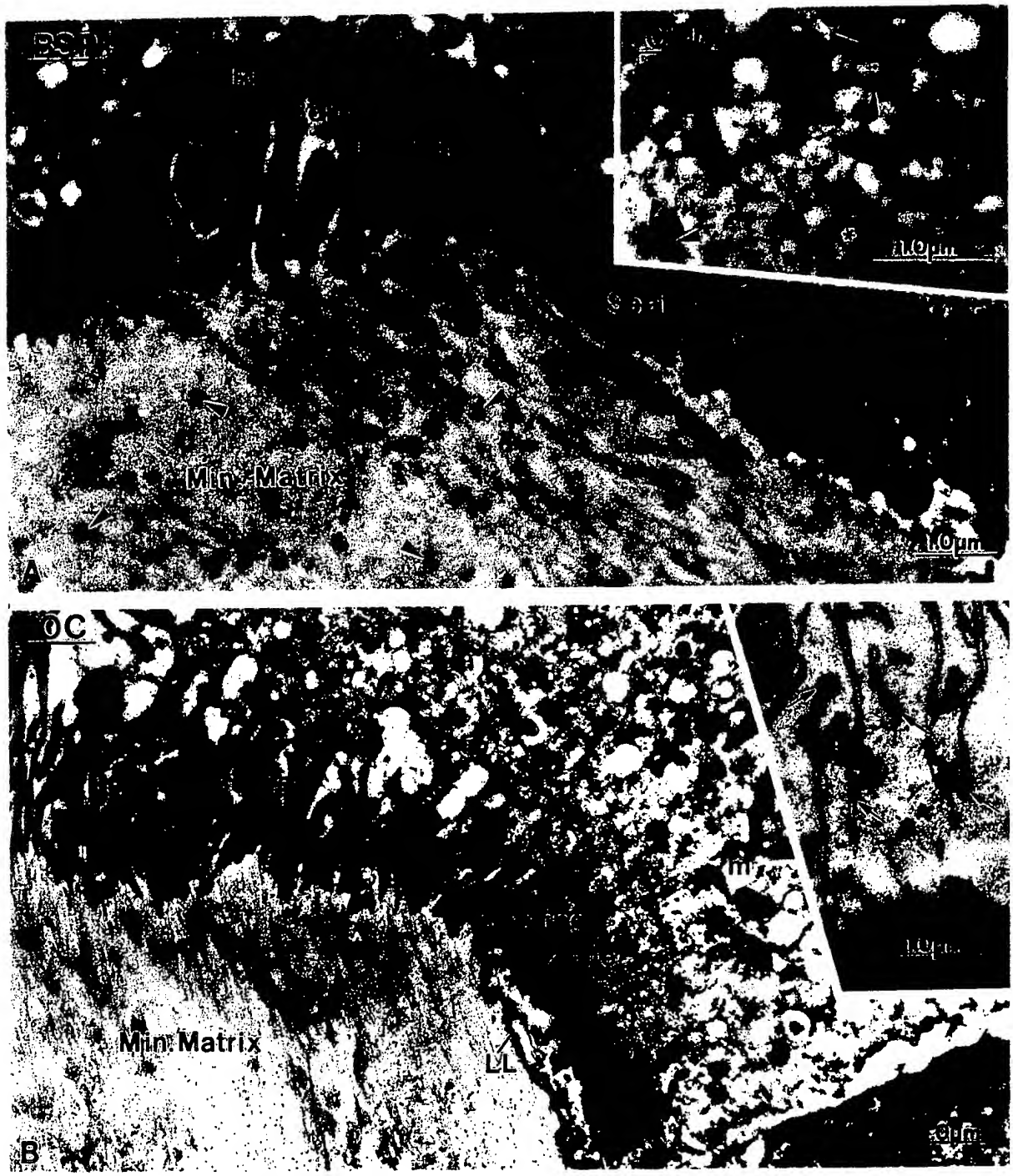

Figure 5 Micrographs illustrating the distribution of bone sialoprotein (BSP), osteocalcin (OC), and osteopontin (OPN) in areas of bone resorption. The osteoclasts show either (A) poorly developed or (B) seemingly normal ruffled borders. Labeling for BSP is mainly found over patches of electron-dense matrix (arrowheads) among the collagen of the mineralized matrix (Min. Matrix), whereas, with the antibody used, OC immunoreactivity occasionally shows a more diffuse distribution. A lamina limitans (LL) is not always present in the region where osteoclasts appose bone, particularly when they exhibit incomplete ruffled borders. (Inset in A) Patches of organic matrix (arrowheads), immunoreactive for (OPN), are occasionally observed within what appears to be partially degraded collagenous matrix (asterisks) and pit-like membrane invaginations associated with poorly developed borders. (Inset in B) Crystallites (arrows) are sometimes observed within the membrane infolding of well-developed ruffled borders. m, mitochondria.

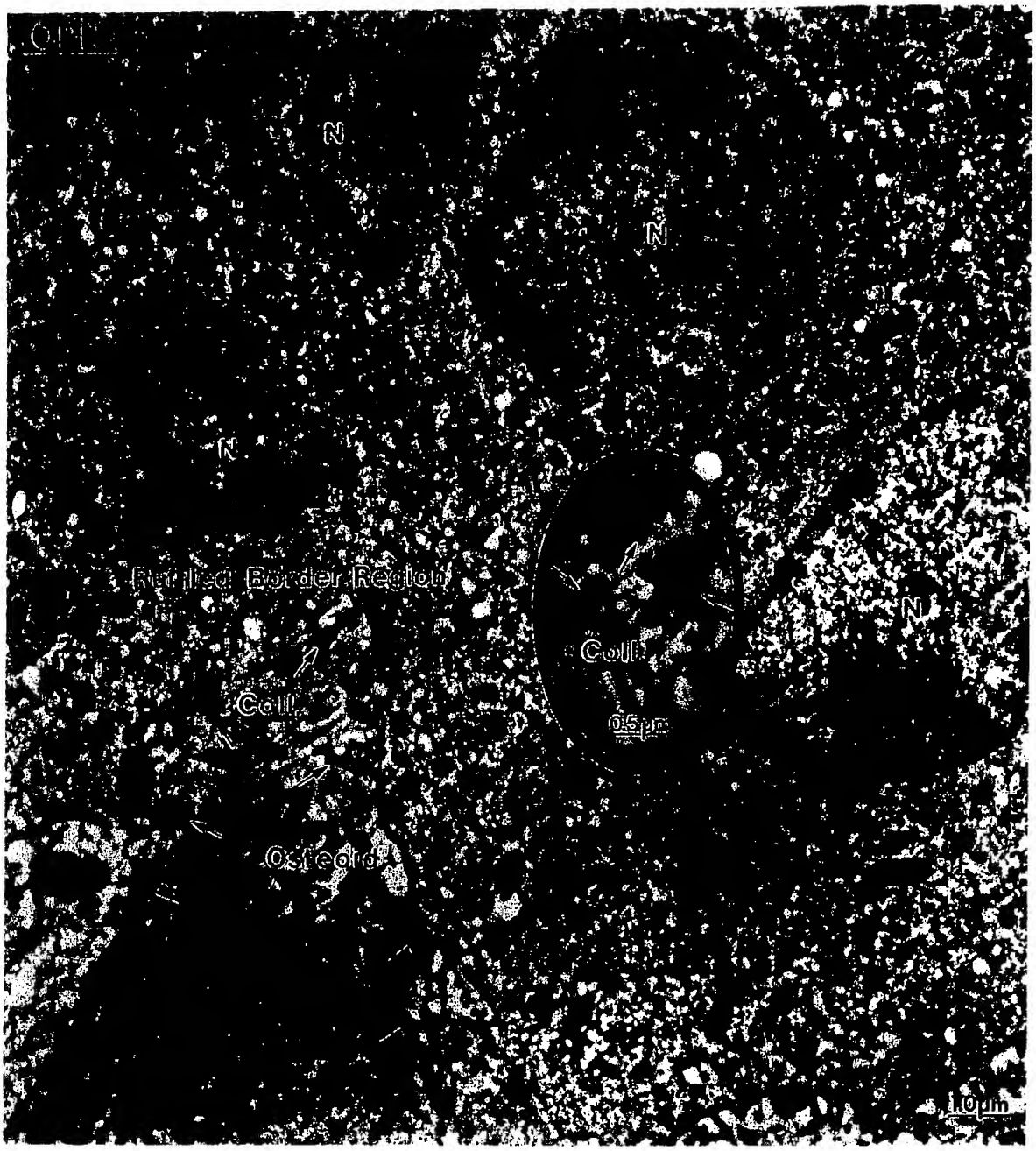

Figure 6 In many cases, the ruffled border region of osteoclasts from hypocalcemic rats is reduced and uncharacteristic, extending coarse cytoplasmic projections (arrows) into the subjacent matrix. Some cells appear to be resorbing osteoid rich in mineralization foci (arrowheads), here immunolabeled for osteopontin (OPN). (Inset) Although collagen fibrils (Coll.) are seen within membrane infoldings of the osteoclasts, fibrils or their fragments have not been discerned in intracellular degradative compartments. N, nucleus.

cells have also been found in normal metaphyseal bone (Bianco et al. 1988; Yamamoto et al. 1996) and in basic multicellular units (BMUs; Baron et al. 1984). In our study, there appeared to be more alkaline phosphatase- and TRAP-positive mononuclear cells on the osteoid surface of calcium-deprived rats than of controls. This observation, albeit with the caveat of being qualitative, suggests that normal levels of interstitial calcium

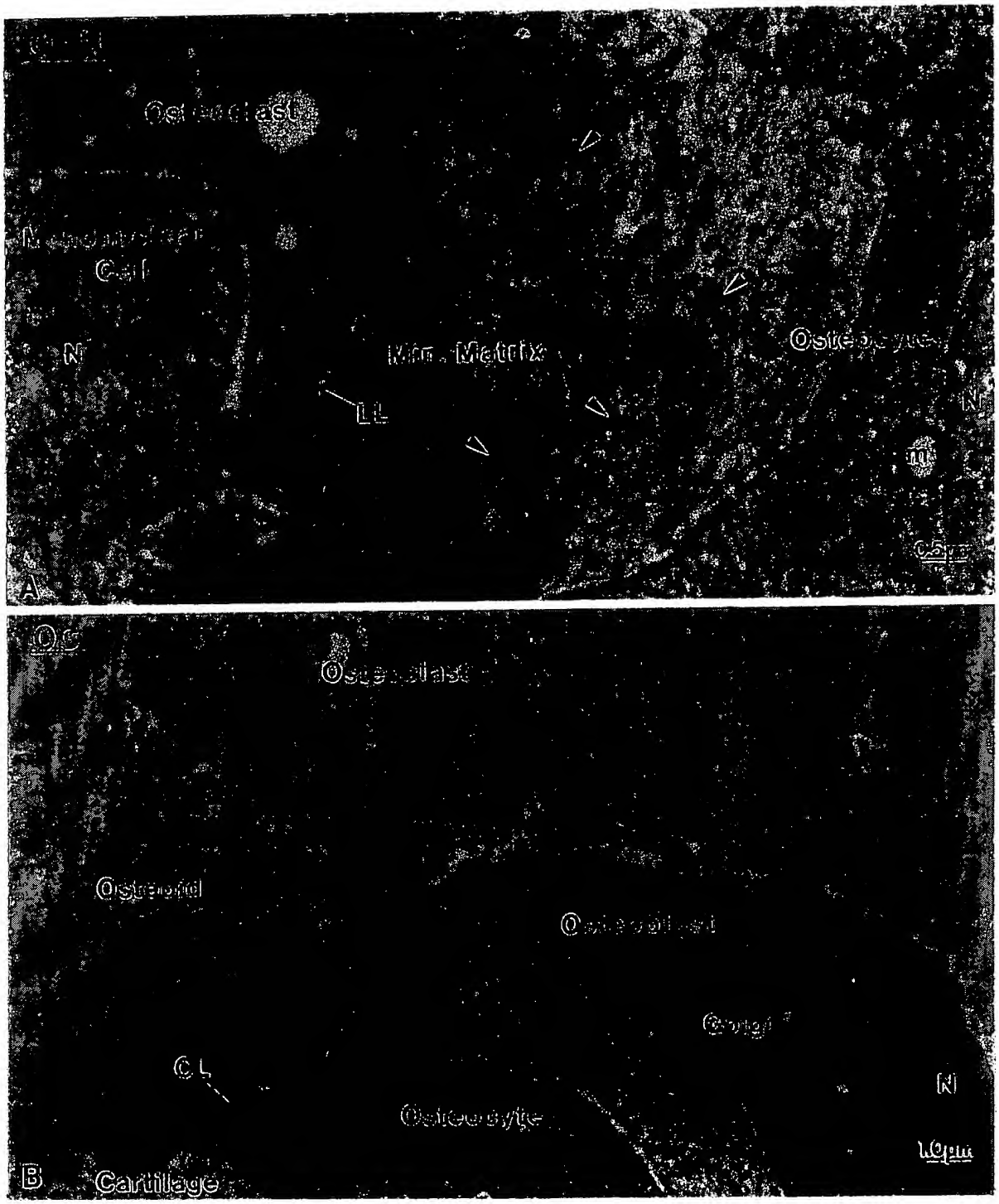

Figure 7 Immunocytochemical preparations with anti-osteopontin (OPN) and anti-osteocalcin (OC) antibodies. Osteoclasts from hypocalcemic rats frequently extend cell extensions between (A) "clear" mononuclear cells with a paucity of organelles or (B) typical osteoblasts, to reach either mineralized bone matrix (Min. Matrix) or osteoid. Note the absence of a well-developed lamina limitans (LL) at the site of contact with the matrix. This suggests that this interfacial matrix layer is not a prerequisite for osteoclast attachment and matrix degradation. Patches of matrix (arrowheads) among the mineralized collagen and the cement line at the bone–cartilage interface are immunoreactive. Golgi, Golgi apparatus; m, mitochondria; N, nucleus.

Figure 8 Cytochemical preparations for TRAP, showing the distribution of reactivity in osteoclasts from hypocalcemic animals. **(A)** This osteoclast extends coarse cytoplasmic extensions (arrows) into the subjacent osteoid matrix. Reaction product is present in vesicular profiles (arrowheads) in the ruffled border zone. **(B)** Intensely reactive vesicles of various sizes (arrowheads) are also found deeper in the cell cytoplasm. Some reactivity is also present along the mitochondrial (m) membrane. mv, matrix vesicle; N, nucleus.

or normal matrix calcification are required for their differentiation into or replacement by true osteoblasts. If these indeed represent intermediate cells of the BMUs, this raises the possibility that calcium ions and/or the degree of matrix calcification may participate in cell signaling and may mediate transition from the reversal to the formation phase. Another element that might modulate this transition is the cement line, whose completion is considered to be followed by the disappearance of the intermediate cells and the appearance of true osteoblasts (Baron et al. 1984). Indeed, the less frequent "coating" of bone surfaces with a lamina limitans is consistent with the abundance of intermediate-like cells in bone of hypocalcemic rats. The presence of mast cells at sites of bone modeling and remodeling may also be implicated in the alterations observed, because it has been suggested that these cells and their mediators participate in the paracrine control, albeit as one of several redundant mechanisms, for recruitment of osteoclast and osteoblast precursors (Silberstein et al. 1991). In this regard, both heparin and histamine are known to play a role in mediating bone formation and resorption (discussed in Silberstein et al. 1991; Muir et al. 1997).

The inconsistent presence of a lamina limitans at sites where osteoclasts were apposed to the bone surface in hypocalcemic rats suggests that these cells are not obligatorily dependent on this interfacial structure for adherence to bone surfaces and for matrix degradation. In this context, it has been shown that osteoclasts can bind to native Type I collagen via $\alpha_2\beta_1$ integrin and denatured collagen via $\alpha_v\beta_3$ integrin (Helfrich et al. 1996), which may in part explain their frequent interaction with osteoid. It may be that, under normal conditions, proteins constituting the lamina limitans lead to a "coordinated" resorptive activity rather than the more "opportunistic" behavior that may take place during the intense bone turnover triggered by the significant reduction of serum calcium.

Another distinctive feature was that cement lines at the bone–calcified cartilage interface sometimes appeared to be thicker than those of control rats. These interfacial lines are believed to derive mainly from the differential deposition of matrix constituents by osteoblasts at the beginning and end of the bone-forming cycle (discussed in McKee and Nanci 1996). The increase in their thickness suggests that the initial upregulation of noncollagenous matrix proteins may have persisted for a longer period of time. Alternatively, extracellular matrix events may have been affected, leading to a looser interaction between the various components constituting cement lines. It has also been

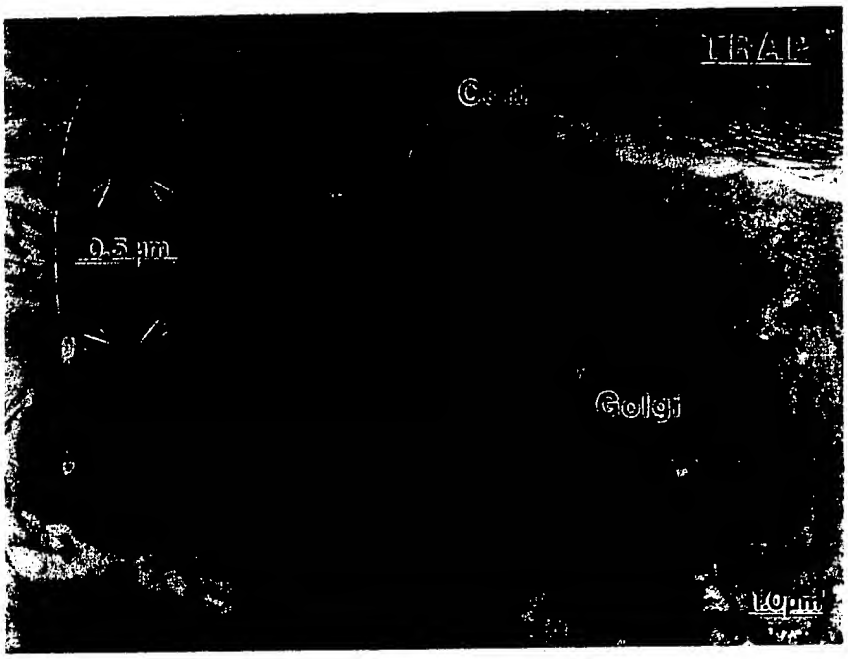

Figure 9 Despite the readily apparent TRAP activity detected by light microscopy in osteoblasts from hypocalcemic rats, at the electron microscopic level cells exhibited only a few weakly reactive granules (arrowheads). Coll., collagen fibrils; Golgi, Golgi apparatus.

proposed that circulating noncollagenous bone matrix proteins may contribute to the formation of cement lines (Nanci et al. in press; Van den Bos et al. 1999). Any increase in their availability in tissue fluids, resulting from impaired mineralization, could also contribute to increasing the thickness of some cement lines.

The intracellular organization of osteoclasts in hypocalcemic rats resembled that of controls. However, they often showed incomplete or poorly formed ruffled borders. The occasional presence of crystallites within the membrane infoldings of the ruffled border in both hypocalcemic and control rats is perplexing, considering the acid pH at this site. Most osteoclasts in calcium-deficient animals exhibited widespread TRAP activity, even when located close to osteoid, suggesting that they can degrade uncalcified bone matrix. Osteoclast-mediated degradation of uncalcified collagen fibrils has also been reported in severe primary hyperparathyroidism (Bonucci et al. 1978). Collagen fibrils were intimately associated with the ruffled border of osteoclasts but were not detected morphologically within intracellular degradative compartments. Unlike fibroblasts, which can endocytose collagen fibrils and degrade them intracellularly (Everts and Beertsen 1987), matrix degradation by osteoclasts is generally believed to occur extracellularly (Väänänen 1996; reviewed in Katsunuma 1997; Nesbitt and Horton 1997). However, it has recently been demonstrated that there is intracellular trafficking of matrix components and/or their fragments released during extracellular enzymatic activity and that these are then transcytosed to the basolateral membrane (Nesbitt and Horton 1997).

TRAP activity was also detected in osteocytes, especially those located near osteoclasts, as previously reported in cases of hyperparathyroidism (Bianco and Bonucci 1991). Osteocytes may therefore also exhibit osteolytic activity, supporting the concept of perios-teocytic osteolysis (reviewed in Bonucci 1990). However, it must be noted that, as for tartrate-sensitive acid phosphatase (TSAP) activity (Wergedal and Baylink 1969), TRAP activity varies inversely with the distance of osteocytes from osteoclasts. The intralacunar TRAP activity detected may therefore not necessarily all derive from osteocytes but may result from the diffusion of the enzyme from the osteoclast towards the osteocyte, establishing a diffusion gradient.

In conclusion, a calcium-free diet administered to young, growing rats reduced the serum calcium level

Figure 10 Mineralized tissue preparations immunolabeled for bone sialoprotein (BSP) and osteopontin (OPN). Both noncollagenous matrix proteins essentially co-localize at the same sites in bone. (A) Overview of the bone matrix deposited onto a calcified cartilage spicule at a serum calcium level half that of normal rats. The bone matrix shows many mineralization foci (arrowheads) but the collagen (Coll.) does not appear mineralized. (Insets) Higher magnifications of the labeling over the cement line (CL) at the bone–cartilage interface and over mineralization foci. (B–D) The bone forming sequence on the calcified cartilage in hypocalcemic rats. (B) Differential secretion by osteoblasts re-

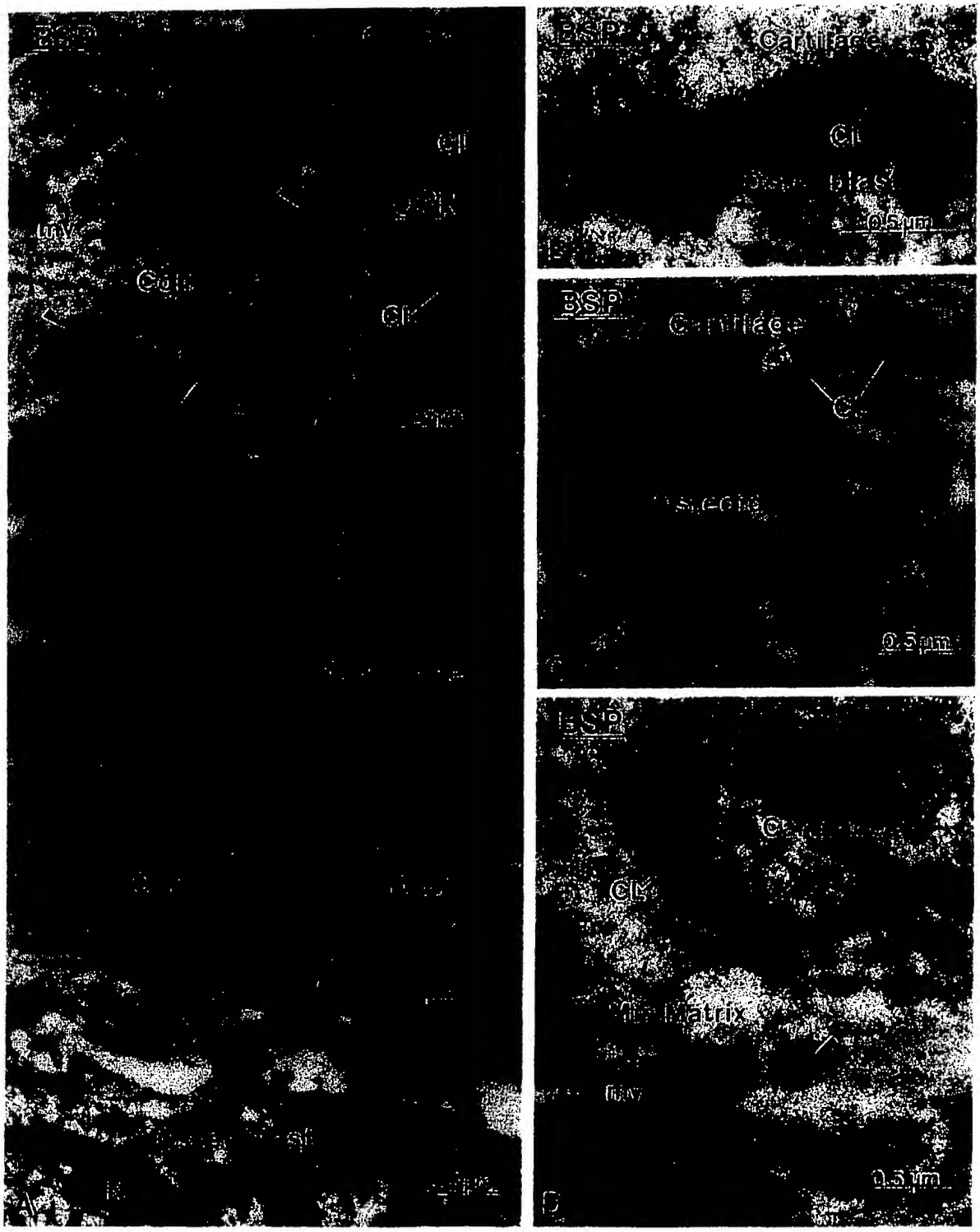

sults in the preferential deposition of BSP and OPN to form a cement line on the calcified cartilage. Because these two noncollagenous proteins are found in blood and tissue fluids, any contribution by circulating proteins to the cement line cannot be excluded. (C) Collagen production is then upregulated to form osteoid (D) which, in the presence of matrix vesicles (mv) and additional noncollagenous bone matrix proteins, will gradually mineralize. N, nucleus.

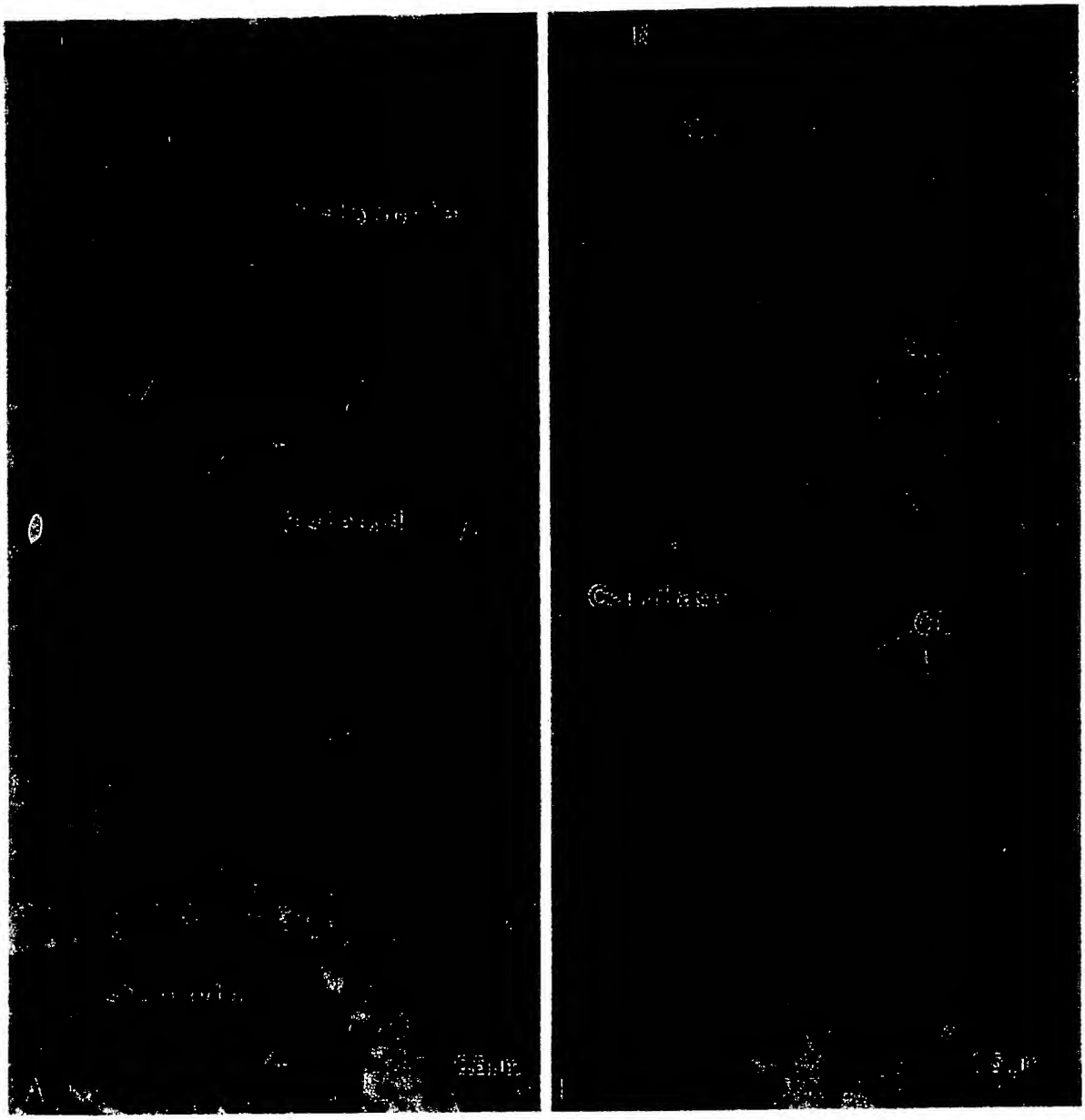

Figure 11 Immunocytochemical preparations for osteopontin (OPN). (A) In hypocalcemic rats, the osteoid layer is thicker and shows many mineralization foci (arrowheads), rich in osteopontin. Osteocytes are found throughout this layer of incompletely mineralized bone matrix. (B) In the primary spongiosa, the cement line (CL) at the interface between calcified cartilage and forming bone often appears thickened compared to controls (inset). N, nucleus.

to about half of normal values but did not significantly change bone volume. Osteoid volume, surface, and thickness increased. There were many mineralization foci in the widened osteoid seam, suggesting aborted attempts at mineralization. These were conspicuously immunoreactive for BSP, OC, and OPN. Bone turnover was increased and osteoblasts were hyperplastic. Most osteoblasts showed TRAP and alkaline phosphatase activity, thus resembling the BMU intermediate cells. Osteoclasts were all intensely stained for TRAP, showed poorly developed ruffled borders, and appeared to digest both calcified and uncalcified bone matrix. Although the alterations observed must take into consideration the effects of both calcium de-

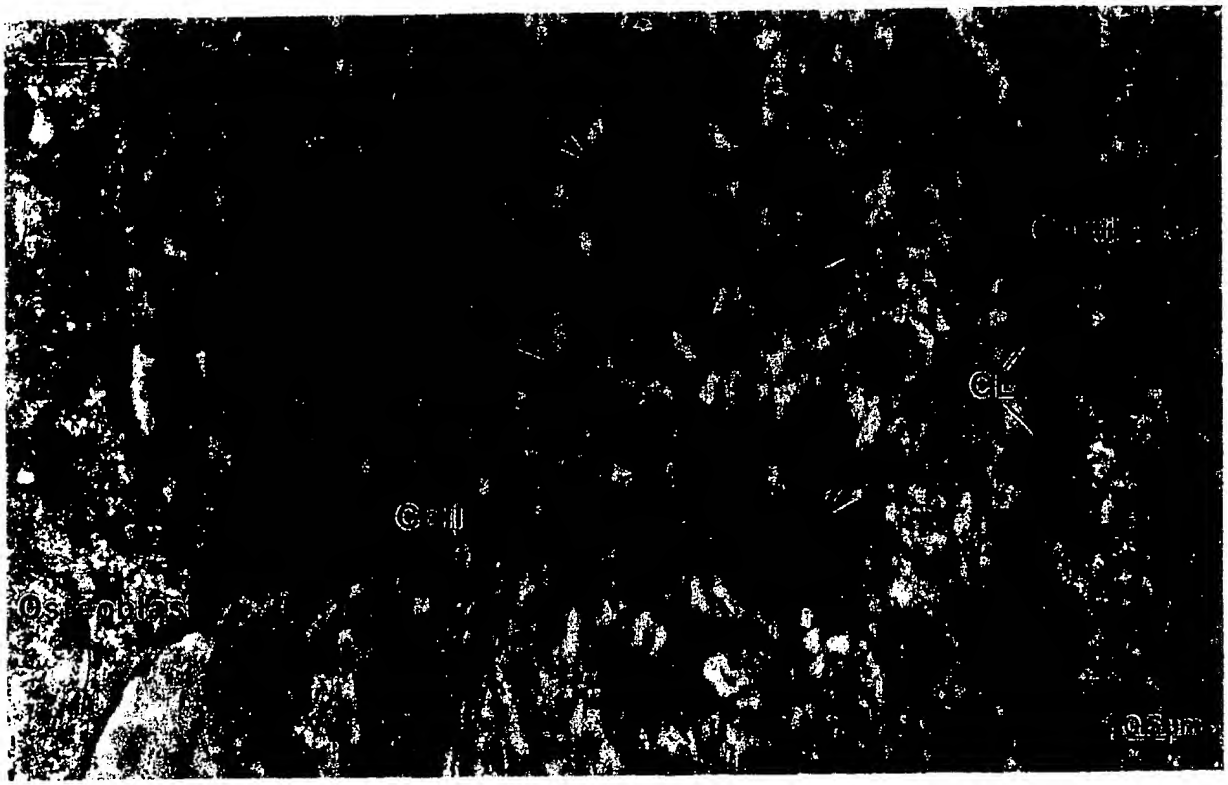

Figure 12 Layer of poorly mineralized bone deposited on calcified cartilage in a hypocalcemic rat. Labeling with an antibody to osteocalcin (OC) is observed over patches (arrowheads) of the afibrillar matrix among the collagen fibrils (Coll.) and which forms the cement line (CL) at the bone–cartilage interface.

ficiency and growth, taken together the data suggest that severe hypocalcemia in young rats induces an osteomalacia-like state which, as is often the case, is characterized by bone changes caused by compensatory secondary hyperparathyroidism.

Acknowledgments

Supported by grants from the Medical Research Council of Canada and the Ministry of University and Scientific and Technological Research (MURST) of Italy. P. Mocetti was the recipient of a fellowship from the Québec Ministry of Education.

We are grateful to Dr L.W. Fisher (National Institutes of Health; Bethesda, MD) for supplying the LF-87 BSP antibody, to Dr P.V. Hauschka (Harvard University; Boston, MA) for the OC antibody, to Dr R. Lepage (Hôpital St-Luc, Montreal, QC) for the biochemical analyses of blood samples, and to M. Fortin for diligent technical and photographic assistance.

Literature Cited

Baron R, Vignery A, Horowitz M (1984) Lymphocytes, macrophages and the regulation of bone remodeling. In Peck WA, ed. Bone and Mineral Research. Annual 2. Amsterdam, Elsevier, 175–243

Bendayan M (1995) Colloidal gold post-embedding immunocytochemistry. Prog Histochem Cytochem 29:1–159

Bendayan M, Nanci A, Kan FWK (1987) Effect of tissue processing on colloidal gold cytochemistry. J Histochem Cytochem 35:983–996

Bianco P, Ballanti P, Bonucci E (1988) Tartrate-resistant acid phosphatase activity in rat osteoblasts and osteocytes. Calcif Tissue Int 43:167–171

Bianco P, Bonucci E (1991) Endosteal surfaces in hyperparathyroidism: an enzyme cytochemical study on low-temperature-processed, glycol-methacrylate-embedded bone biopsies. Virchows Arch [A] 419:425–431

Bianco P, Ponzi A, Bonucci E (1984) Basic and "special" stains for plastic sections in bone marrow histopathology, with special reference to May-Grunwald Giemsa and enzyme histochemistry. Basic Appl Histochem 28:265–279

Bianco P, Riminucci M, Silvestrini G, Bonucci E, Termine JD, Fisher LW, Gehron Robey P (1993) Localization of bone sialoprotein (BSP) to Golgi and post-Golgi secretory structures in osteoblasts and to discrete sites in early bone matrix. J Histochem Cytochem 41:193–203

Bloom MA, Domm LV, Nalbandov AV, Bloom W (1958) Medullary bone of laying chickens. Am J Anat 102:411–453

Bonucci E (1990) The ultrastructure of the osteocyte. In Bonucci E, Motta PM, eds. Ultrastructure of Skeletal Tissues. Boston, Kluwer Academic Publishers, 223–237

Bonucci E, Lo Cascio V, Adami S, Cominacini L, Galvanini G, Scuro A (1978) The ultrastructure of bone cells and bone matrix in human primary hyperparathyroidism. Virchows Arch [A] 379:11–23

Bonucci E, Silvestrini G, Bianco P (1992) Extracellular alkaline phosphatase activity in mineralizing matrices of cartilage and bone: ultrastructural localization using a cerium-based method. Histochemistry 97:323–327

Clark SA, Ambrose WW, Anderson TR, Terrell RS, Toverud SU (1989) Ultrastructural localization of tartrate-resistant, purple acid phosphatase in rat osteoclasts by histochemistry and immunocytochemistry. J Bone Miner Res 4:399–405

de Bernard B, Stagni N, Camerotto R, Vittur F, Zanetti M, Zambonin Zallone A, Teti A (1980) Influence of calcium depletion on medullary bone of laying hens. Calcif Tissue Int 32:221–228

Dempster DW (1992) Bone remodeling. In Coe FL, Favus MJ, eds. Disorders of Bone and Mineral Metabolism. New York, Raven Press, 355–380

de Winter FR, Steendijk R (1975) The effect of a low-calcium diet in lactating rats: observations on the rapid development and repair of osteoporosis. Calcif Tissue Res 17:303–316

Everts V, Beertsen W (1987) The role of microtubules in the phagocytosis of collagen by fibroblasts. Coll Relat Res 7:1–15

Frens G (1973) Controlled nucleation for the regulation of particle size in monodispersed gold suspensions. Nature [Phys Sci] 241: 20–22

Hauschka PV, Frenkel J, DeMuth R, Gundberg CM (1983) Presence of osteocalcin and related higher molecular weight 4-carboxyglutamic acid-containing proteins in developing bone. J Biol Chem 258:176–182

Helfrich MH, Nesbitt SA, Lakkakorpi PT, Barnes MJ, Bodary SC, Shankar G, Mason WT, Mendrick DL, Väänänen HK, Horton MA (1996) β_1 Integrins and osteoclast function: involvement in collagen recognition and bone resorption. Bone 19:317–328

Jowsey J, Gershon–Cohen J (1964) Effect of dietary calcium levels on production and reversal of experimental osteoporosis in cats. Proc Soc Exp Biol Med 116:437–441

Katsunuma N (1997) Molecular mechanisms of bone collagen degradation in bone resorption. J Bone Miner Metab 15:1–8

Liu C-C, Baylink DJ (1984) Differential response in alveolar bone osteoclasts residing at two different bone sites. Calcif Tissue Int 36:182–188

Liu C-C, Rader JL, Gruber H, Baylink DJ (1982) Acute reduction in osteoclast number during bone repletion. Metab Bone Dis Relat Res 4:201–209

McKee MD, Farach-Carson MC, Butler WT, Hauschka PV, Nanci A (1993) Ultrastructural immunolocalization of noncollagenous (osteopontin and osteocalcin) and plasma (albumin and α_2HS-glycoprotein) proteins in rat bone. J Bone Miner Res 8:485–496

McKee MD, Nanci A (1995) Postembedding colloidal-gold immunocytochemistry of noncollagenous proteins in mineralized tissues. Microsc Res Tech 31:44–62

McKee MD, Nanci A (1996) Osteopontin at mineralized tissue interfaces in bone, teeth, and osseointegrated implants: ultrastructural distribution and implications for mineralized tissue formation, turnover, and repair. Microsc Res Tech 33:141–164

Midura RJ, McQuillan DJ, Benham KJ, Fisher LW, Hascall VC (1990) A rat osteogenic cell line (UMR 106-01) synthesizes a highly sulfated form of bone sialoprotein. J Biol Chem 265: 5285–5291

Muir JM, Hirsh J, Weitz JI, Andrew M, Young E, Shaughnessy SG (1997) A histomorphometric comparison of the effects of heparin and low-molecular-weight heparin on cancellous bone in rats. Blood 89:3236–3242

Nanci A (1999) Content and distribution of noncollagenous matrix proteins in bone and cementum: relationship to speed of formation and collagen packing density. J Struct Biol 126:256–269

Nanci A, Ahluwalia JP, Zalzal S, Smith CE (1989) Cytochemical and biochemical characterization of glycoproteins in forming and maturing enamel of the rat incisor. J Histochem Cytochem 37:1619–1633

Nanci A, McCarthy GF, Zalzal S, Clokie CML, Warshawsky H, McKee MD (1994) Tissue response to titanium implants in the rat tibia: ultrastructural, immunocytochemical and lectin-cytochemical characterization of the bone-titanium interface. Cells Mater 4:1–30

Nanci A, Mocetti P, Sakamoto Y, Kunikata M, Lozupone E, Bonucci E (2000) Morphological and immunocytochemical analyses on the effects of diet-induced hypocalcemia on enamel maturation in the rat incisor. J Histochem Cytochem 48:1043–1057

Nanci A, Zalzal S, Fortin M, Mangano C, Goldberg HA (2000) Incorporation of circulating bone matrix proteins by implanted hydroxyapatite and at bone surfaces: implications for cement line formation and structuring of biomaterials. In Davies JE, ed. Bone Engineering. Toronto, em^2, Inc. (In Press)

Nanci A, Zalzal S, Gotoh Y, McKee MD (1996) Ultrastructural characterization and immunolocalization of osteopontin in rat calvarial osteoblast primary culture. Microsc Res Tech 33:214–231

Neiss WF (1984) Electron staining of the cell surface coat by osmium-low ferrocyanide. Histochemistry 80:231–242

Nesbitt SA, Horton MA (1997) Trafficking of matrix collagens through bone-resorbing osteoclasts. Science 276:266–269

Ohya K (1994) Rats fed with a low-calcium diet as an in vivo experimental model for bone resorption. In Ogura H, ed. Pharmacological Approach to the Study of the Formation and the Resorption Mechanism of Hard Tissues. Tokyo, Ishiyaku Euroamerica, 93–113

Ornoy A, Wolinsky I, Guggenheim K (1974) Structure of long bones of rats and mice fed a low calcium diet. Calcif Tissue Res 15:71–76

Parfitt AM (1990) Osteomalacia and related disorders. In Avioli LV, Krane SM, eds. Metabolic Bone Disease and Clinically Related Disorders. 2nd ed. Philadelphia, WB Saunders, 329–396

Parfitt AM, Drezner MK, Glorieux FH, Kanis JA, Malluche H, Meunier PJ, Ott SM, Recker RR (1987) Bone histomorphometry: standardization of nomenclature, symbols, and units. J Bone Miner Res 2:595–610

Persson P, Gagnemo–Persson R, Håkanson R (1993) The effect of high or low dietary calcium on bone and calcium homeostasis in young male rats. Calcif Tissue Int 52:460–464

Pettifor JM, Marie PJ, Sly MR, du Bruyn DB, Ross F, Isdale JM, de Klerk WA, van der Walt WH (1984) The effect of differing dietary calcium and phosphorus contents on mineral metabolism and bone histomorphometry in young vitamin D-replete baboons. Calcif Tissue Int 36:668–676

Riminucci M, Silvestrini G, Bonucci E, Fisher LW, Gerhon Robey P, Bianco P (1995) The anatomy of bone sialoprotein immunoreactive sites in bone as revealed by combined ultrastructural histochemistry and immunohistochemistry. Calcif Tissue Int 57:277–284

Robinson JM, Karnovsky MJ (1983) Ultrastructural localization of several phosphatases with cerium. J Histochem Cytochem 31: 1197–1208

Salomon CD (1972) Osteoporosis following calcium deficiency in rats. Calcif Tissue Res 8:320–333

Salomon CD, Volpin G (1970) Fine structure of bone resorption in experimental osteoporosis caused by calcium deficient diet in rats. An electron microscopic study of compact bone. Calcif Tissue Res 4:80–82

Scherft JP, Groot CG (1990) The electron microscopic structure of the osteoblast. In Bonucci E, Motta PM, eds. Ultrastructure of Skeletal Tissues. Boston, Kluwer Academic Publishers, 209–222

Shen V, Birchman R, Xu R, Lindsay R, Dempster DW (1995) Short-term changes in histomorphometric and biochemical turnover markers and bone mineral density in estrogen- and/or dietary calcium-deficient rats. Bone 16:149–156

Silberstein R, Melnick M, Greenberg G, Minkin C (1991) Bone remodeling in W/W^v mast cell deficient mice. Bone 12:227–236

Sissons HA, Kelman GJ, Marotti G (1984) Mechanisms of bone resorption in calcium-deficient rats. Calcif Tissue Int 36:711–721

Stauffer M, Baylink D, Wergedal J, Rich C (1972) Bone repletion in calcium deficient rats fed a high calcium diet. Calcif Tissue Int 9:163–172

Stauffer M, Baylink D, Wergedal J, Rich C (1973) Decreased bone formation, mineralization, and enhanced resorption in calcium-deficient rats. Am J Physiol 225:269–276

Thomas ML, Simmons DJ, Kidder L, Ibarra MJ (1991) Calcium metabolism and bone mineralization in female rats fed diets marginally sufficient in calcium: effects of increased dietary calcium intake. Bone Miner 12:1–14

Thompson ER, Baylink DJ, Wergedal JE (1975) Increases in number and size of osteoclasts in response to calcium or phosphorus deficiency in the rat. Endocrinology 97:283–289

Väänänen HK (1996) Osteoclast function: biology and mechanisms. In Bilezikian JP, Raisz LG, Rodan GA, eds. Principles of Bone Biology. San Diego, Academic Press, 103–114

Van den Bos T, Bronckers ALJJ, Goldberg HA, Beertsen W (1999) Blood circulation as a source of osteopontin in acellular extrinsic fiber cementum and other mineralizing tissues. J Dent Res 78: 1688–1695

Warshawsky H, Moore G (1967) A technique for the fixation and decalcification of rat incisors for electron microscopy. J Histochem Cytochem 15:542–549

Weinreb M, Rodan GA, Thompson DD (1991) Immobilization-related bone loss in the rat is increased by calcium deficiency. Calcif Tissue Int 48:93–100

Wergedal JE, Baylink DJ (1969) Distribution of acid and alkaline phosphatase activity in undemineralized sections of the rat tibial diaphysis. J Histochem Cytochem 17:799–806

Yamamoto T, Yamagata A, Nagai H (1996) A histochemical study of tartrate-resistant acid phosphatase activity in rat osteoblasts. Acta Histochem Cytochem 29:221–225